Monatshefte für Chemie - Chemical Monthly (2023) 154:1225–1233
https://doi.org/10.1007/s00706-023-03126-8

ORIGINAL PAPER

Quantification of ferulic acid using square-wave voltammetric method at an unmodified boron-doped diamond electrode

Pınar Talay Pınar[1] · Hemn A. H. Barzani[2] · Hoshyar Saadi Ali[3,4] · Yavuz Yardım[1]

Received: 4 July 2023 / Accepted: 28 August 2023 / Published online: 29 September 2023

Abstract

For the first time, a boron-doped diamond electrode was employed in square-wave voltammetry for the sensitive and selective measurement of ferulic acid (FA). The impact of the electrode's pretreatment procedure on the current response was investigated, leading to the discovery that the consecutive pretreatment approach yielded the most optimal signal results. This determination was made upon observing that the highest quality signal could be obtained through this method. The electrochemical oxidation of FA was studied in aqueous media on a cathodically pretreated boron-doped diamond electrode. FA was shown to have two sets of oxidation/reduction peaks when tested in aqueous solutions using cyclic voltammetry. Diffusion governs the electrode process, which is pH-dependent. In 0.1 mol dm^{-3} H_2SO_4, the calibration curves were linear for FA peak over dynamic ranges of 5.1×10^{-7}–4.1×10^{-5} mol dm^{-3}, via a detection limit of 1.5×10^{-7} mol dm^{-3}. The practical applicability of the developed methodology was tested in the commercial ampoule formulation of FA. The method can be used instead of other analytical methods because it is fast, easy to use, and cheap, has a wide calibration range, and gives consistent results.

Graphical abstract

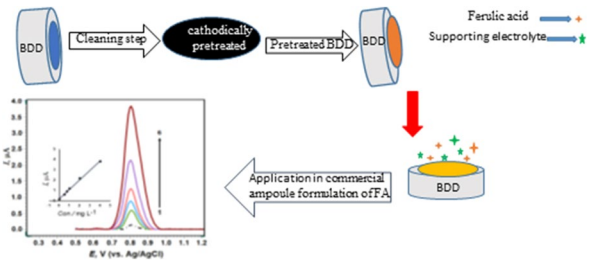

Keywords Ferulic acid · Voltammetry · Boron-doped diamond electrode · Injection sample

Introduction

Antioxidants are molecules needed by most creatures because they protect cells from the oxidative damage induced by free radicals, which has been linked to several illnesses in humans, including cardiovascular, cancer disease, and cataracts [1]. The use of natural antioxidants has gained a lot of attention in recent years. The phenolic content of plants, one type of natural antioxidant, has been widely credited with the plants' antioxidant capabilities. This highlights the possible significance of plants rich in phenolic acids as a source of natural antioxidants [2].

✉ Yavuz Yardım
yavuzyardim2002@yahoo.com

1 Faculty of Pharmacy, Department of Analytical Chemistry, Van Yuzuncu Yil University, 65080 Van, Turkey

2 Department of Pharmacy, Aynda Private Technical Institute, 44001 Erbil, Iraq

3 Department of Medical Laboratory Science, College of Science, Knowledge University, Kirkuk, 44001 Erbil, Iraq

4 Faculty of Science, Department of Analytical Chemistry, Van Yuzuncu Yil University, 65080 Van, Turkey

3-Methoxy-4-hydroxycinnamic acid, often known as ferulic acid (FA, Fig. 1), is a naturally occurring phenolic compound discovered in a broad numerous of intricate matrices, including fruits, packaged fruit juices, vegetables, beverages containing alcohol, and several traditional Chinese medicinal herbs [3, 4]. Several hydroxycinnamic acids and flavonoids, including FA, caffeic acid, and sinapic acid, have been investigated for their potential as antioxidants because of their natural origin. These compounds can scavenge superoxide anions, peroxyl anions, hydroxyl radicals, and other oxidative species [5]. FA has been studied for its ability to prevent cell death, inflammation, thrombosis, diabetes, ulcers, blood clotting, hemolysis, chemotherapy, and viruses. As a result, it is often utilized to prevent infection in artificial joints [6–10]. FA is a key metabolite of chlorogenic acids and plays a significant function in human health [11, 12]. FA has a strong antioxidant impact and can help eliminate harmful free radicals [13]. Furthermore, it has a potent analgesic impact and is recommended to relieve neuropathic pain [12, 14]. The antioxidant capabilities of FA and its applications in the food business, pharmaceutical industry, and cosmetics industry have been the subject of extensive investigation [15–17]. One of the most pressing concerns of modern esthetic medicine and cosmetics is anti-aging skin care. FA is an effective antioxidant chemical. Found in the cosmetics industry, FA has also been utilized as a stabilizer for other prominent antioxidants such as vitamin C and vitamin E [18]. New evidence suggests, nevertheless, that this molecule is an integral part of the intracellular antioxidant defense mechanisms. That is why FA is commonly found in anti-aging skin care products [19, 20]. Cosmetics containing it are used to reduce the appearance of age spots due to their ability to inhibit the primary enzyme involved in melanin production [21].

There are several proven analytical techniques for identifying FA in its unprocessed state, pharmaceutical products, and biological samples, for instance, voltammetry [22–35], spectrophotometry [36, 37], capillary electrophoresis (CE) [38], thin layer chromatography (TLC) [2, 39, 40], and high-performance liquid chromatography (HPLC) [41–47]. However, as of now, no study has been encountered in the literature regarding the voltammetric analysis of FA using an unmodified electrode. Electroanalytical approaches, particularly voltammetric methods, may be good options owing to their user-friendliness, low device price, fast analysis, use of low-toxicity reagents (typically aqueous buffer solutions), suitable sensitivity, as well as good selectivity relying on the type of working electrode. Another advantage of voltammetry over non-electrochemical methods is its ability to provide insights into the oxidation–reduction behavior of targeted substances through redox-active groups. This understanding is vital for developing novel approaches to treat and/or alleviate the toxic effects of these materials [48]. To enhance the reliability of FA detection using the voltammetric method, the development of an improved electrode material is necessary. Therefore, the BDD electrode is chosen for this analysis, as it offers greater benefits than any alternative. The BDD electrode offers a wide potential range compared to other electrode materials, encompassing diverse metals like gold and platinum, along with conventional sp2 carbon substances such as carbon paste, pyrolytic graphite, and glassy carbon. Distinctive features include a strong chemical and physical resistance that maintains signal repetition and a low constant voltammetric background current. Due to the sp3 hybridization of the carbon atoms in the diamond structure, it has poor adsorption of most contaminants. It is important to note that for various analytes, the analytical performance of a BDD electrode (oxygen or hydrogen-terminated surface functionalities) is significantly influenced by three critical variables. Boron doping (which guarantees outstanding shape and electrical conductivity) and non-diamond sp2 carbon (sp2 impurities) alter the kinetics of electron transport, while surface treatments also play a role [49, 50]. This last factor is possibly the most intricate that can affect the electrode surface properties. BDD (commercially available or synthesized in the lab) has a hydrophobic (hydrogen-terminated) surface in its as-prepared state. To make BDD hydrophilic (oxygen halted) and have a considerably negative surface charge depending on the polarization potential and time, it is necessary to apply strong positive potentials during the oxygen-generating reaction (anodic pretreatment, APT). However, by selecting appropriate potentials in the hydrogen production reaction (cathodic pretreatment, CPT), the hydrophobic nature of the BDD surface via its high electrical conductivity may further be demonstrated. Electrochemical pretreatments can improve sensitivity and selectivity and diminish fouling without alerting the BDD surface for any electroanalytical purpose [51–62].

We could not find any research on the electroanalytical detection of FA with a non-modified electrode. The primary purpose of this study is to offer a workable approach for determining FA by employing a voltammetric strategy that is not only sensitive but also selective, in addition to being straightforward to implement in real-world settings. The viability of the procedure was established through the

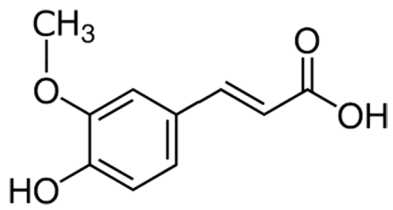

Fig. 1 Chemical structure of ferulic acid

successful application of analyte in a cosmetic formulation while operating under ideal conditions.

Results and discussion

Electrochemical response of FA on the BDD electrode

The electrochemical characteristics of FA were assessed through the CV technique applied to the BDD electrode. Utilizing an impact, the rate of voltage scanning of 100 mV s^{-1}, three sequential CVs for 1.03×10^{-4} mol dm^{-3} of FA were recorded among 0.0 and + 1.40 V in a solution of 0.1 mol dm^{-3} H_2SO_4. FA displayed an anodic peak (well defined) a potential (I_a) of at around + 0.85 V (Fig. 2A). Two reduction waves designated as I_c and II_c were also seen while scanning in the other orientation, at roughly + 0.75 V (poorly defined) and + 0.44 V (well defined), respectively. In addition, during the second and subsequent scans, a new anodic peak (II_a) was recorded at around + 0.67 V. With an increase in the number of scans, the peak height of I_a decreased gradually when the intensity of II_c/II_a slightly increased. These findings suggest that the oxidation peak at I_a is not reversible, while the pair of redox peaks at II_c/II_a is indicative of a redox process. This could be due to the formation of byproducts during the main electrooxidation step. As a result, while sequential CVs were obtained, the main oxidation peak (I_a) was found to decrease, possibly due to the accumulation of FA and/or its oxidation products on the BDD electrode surface, leading to deactivation or fouling. The impact of voltage scan rate (v) on the oxidation peak current of 1.03×10^{-4} mol dm^{-3} FA was worked using a CV approach solution of 0.1 mol dm^{-3} H_2SO_4 at the v of 10–1000 mV s^{-1} (Fig. 2B) to investigate a BDD electrode kinetics. As the scan rate was raised, a little change was seen in the oxidation peak potentials toward higher positive values. The anodic peak currents of FA were raised by increasing the square root of the scan rate ($v^{1/2}$). Equation was used to evaluate that FA's oxidation peak currents are commensurate to the $v^{1/2}$ utilizing the equation; i_p (μA) = 0.306 $\nu^{1/2}$ (mV s^{-1}) − 0.099 (r = 0.998, n = 10).

Hence, it might be considered that the FA oxidation is controlled via a diffusion. To determine the number of electrons (n) participating in the FA oxidation process at the BDD electrode, the n value was calculated using the equation $\alpha n = 47.7/(E_p - E_{p/2})$. In this study, the value of $E_p - E_{p/2}$ was 57 mV. Typically, the α (charge transfer coefficient) is considered to be 0.5 in a completely irreversible electrode process. As a result, the n value was determined to be 1.67 (≈ 2), consistent with the findings reported in a previous study regarding the oxidation process of FA [35]. While the purpose of this study does not include an exhaustive exploration of the mechanism behind FA electrochemical oxidation, an evaluation based on the cyclic voltammograms at the BDD electrode, in addition to considering the voltammetric response of FA at a γ-$CoTe_2$ nanocrystals modified glassy carbon electrode (γ-$CoTe_2$/GCE) in an acidic aqueous solution [35], allows for the tentative proposal of an oxidation mechanism for FA at the BDD electrode (Scheme 1).

Preliminary tests showed that FA induced electrode passivation (particularly at its high concentrations); thus, two pretreatment approaches were investigated for 5.15×10^{-5} mol dm^{-3} FA in 0.1 mol dm^{-3} H_2SO_4 using SWV. An anodic polarization (APT-BDD, oxygen-terminated surface) was first applied to the electrode at + 1.8 V for 180 s. For the second step (cathodically pretreated boron-doped diamond (CPT-BDD), hydrogen-terminated surface), we applied a cathodic polarization of − 1.8 V for 180 s. Initially, CV measurements were recorded at a scan rate of 100 mV s^{-1} for the redox couple of 5×10^{-3} mol dm^{-3} $[Fe(CN)_6]^{3-/4-}$ in 0.1 mol dm^{-3} KCl to assess the impact of both pretreatment methods. For $[Fe(CN)_6]^{3-/4-}$, the discrepancies (E_p) between the oxidation and reduction peaks

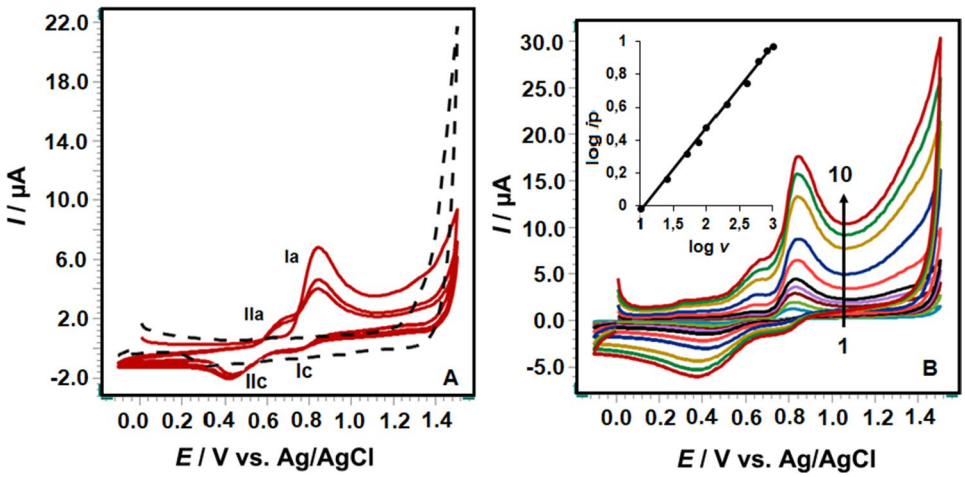

Fig. 2 In (**A**), 1.03×10^{-4} mol dm^{-3} FA in 0.1 mol dm^{-3} H_2SO_4 on BDD electrode is subjected to repeating CVs at a scan rate of 100 mV s^{-1}, whereas in (**B**), CVs are subjected to a range of scan rates (10, 25, 50, 75, 100, 200, 400, 600, 800, and 1000 mV $s.^{-1}$). Background current is shown by dashed lines (**A**). Insets the plots of log i_p vs. log v (**B**)

Scheme 1

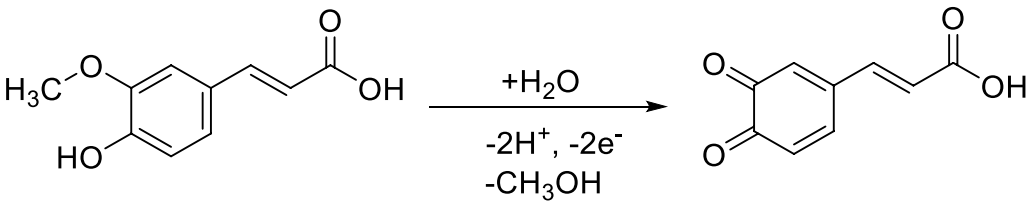

are 111 and 79 mV for APT-BDD and CPT-BDD, respectively. This information is displayed in Fig. 3A. They have slightly greater anodic and cathodic peak currents. Despite the large discrepancy between the observed value of E_p and the expected value of 59 mV for reversible systems, our finding suggests that cathodically pretreated BDD has modestly enhanced surface activity. In addition, as can be observed in Fig. 3B, the current response of FA is greater while the cathodic activation procedure is used as opposed to the anodic one. Note that the BDD electrode used in this investigation, with a diameter of 3 mm and boron content of 1000 ppm, exhibited predominantly hydrophobic characteristics after a minor reduction process.

Nevertheless, pretreatment potentials above + 2.0 V had an unfavorable impact on FA's current susceptibility. Higher positive values had no apparent effect on the oxidation peak current when tested between + 1.8 and + 2.0 V. Therefore, a cathodic pretreatment technique was used to revive the surface of BDD daily. This process involves applying − 1.8 V for 180 s. Voltammetric responses were kept consistent between measurements by employing brief (60 s) polarizations under the same circumstances (at – 1.8 V).

Additional effort was put into determining the impact of supporting electrolytes with varying pH levels to acquire the optimum voltammetric results for analytical justifications. Baseline-adjusted SW voltammograms for the oxidation of 2.58×10^{-5} mol dm^{-3} FA in a potential window of 0.0 V to + 1.2 V are shown in Fig. 4A for a range of BR buffers with pH 2.0–12.0. Between 2.0 and 7.0, the two anodic peaks, I_a and II_a, were measured. As the pH of a solution is increased from 2.0 to 12.0, as shown in Fig. 4A, the oxidation peak moves towards lower potentials.

Figure 4B illustrates the SW voltammograms in several different supporting electrolytes. Using 0.1 mol dm^{-3} H_2SO_4, a phosphate buffer with a pH of 2.5, an acetate buffer with a pH of 4.8, and another phosphate buffer with a pH of 7.4, we were able to generate anodic peak potentials of + 0.793, 0.809, 0.801, and 0.622 V, with peak currents of 5.09, 2.88, 2.14, and 0.98 µA. The peak current was greatest in 0.1 mol dm^{-3} H_2SO_4, as illustrated in Fig. 4A and B. Therefore, these subsequent measurements were performed using this medium for analysis.

Subsequently, attempts were made to optimize the influence of pulse parameters within those circumstances (frequency, $f = 25$–150 Hz; step potential, $\Delta E_s = 8$–16 mV; square-wave amplitude, $\Delta E_{sw} = 30$–80 mV; data not shown). The optimization was carried out by varying just one of many parameters while holding the others constant. Maximum sensitivity was achieved with the following parameters: $f = 100$ Hz; $\Delta E_s = 10$ mV; and $\Delta E_{sw} = 50$ mV.

Quantification of FA on boron-doped diamond electrode

Analytical efficacy was assessed by looking at the concentration oxidation peaks of FA in light of the results reported

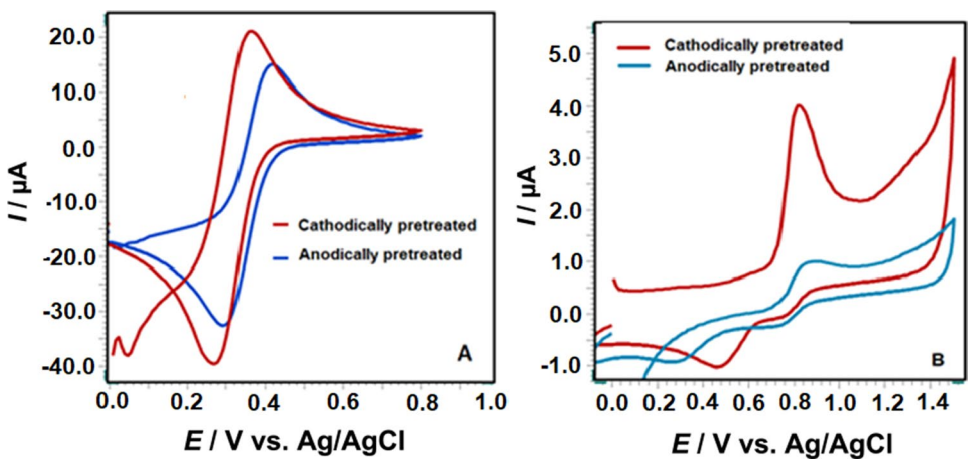

Fig. 3 Cyclic voltammograms of 5.15×10^{-5} mol dm^{-3} FA at a scan rate of 100 mV s^{-1} in 0.1 mol dm^{-3} KCl (**A**) and H_2SO_4 (**B**) on the BDD electrode cathodically or anodically pretreated

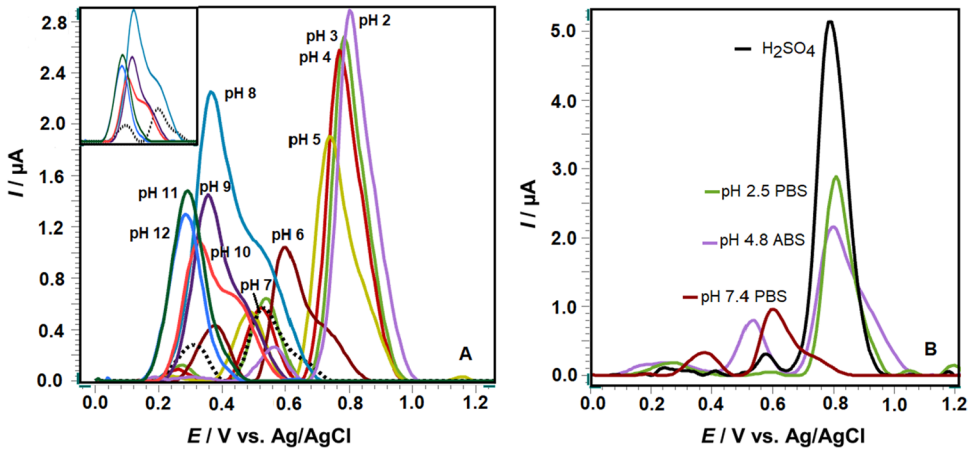

Fig. 4 **A** SW voltammogram of 2.58×10^{-5} mol dm^{-3} FA in BR buffer (pH 2.0–12.0) and **B** SW voltammograms of the same concentration (in a variety of supporting electrolytes) at a range of pH values (**B**). Electrode, CPT-BDD; SWV settings of 50 Hz frequency, 8 mV scan increment, and 30 mV pulse amplitude

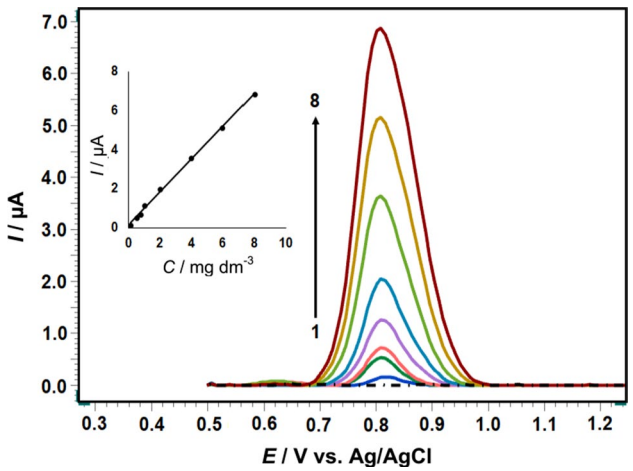

Fig. 5 SW voltammograms for FA levels of 5.15×10^{-7}–4.12×10^{-5} mol dm^{-3} for oxidation peak in 0.1 mol dm^{-3} H_2SO_4. Background current is depicted by the dotted lines. The associated FA quantification calibration charts are displayed in the inset. Electrode, CPT-BDD; SWV parameters: frequency, 100 Hz; scan increment, 10 mV; pulse amplitude, 50 mV

thus far. Figure 5 displays the voltammetric responses, and Table 1 describes the associated analytic parameters. Limits of detection (LOD) and quantification (LOQ) were established based on analytical curve data as follows; three times the standard deviation of the peak currents (ten runs) for the lowest concentration in the related linearity range divided by the slope of each of the calibration curves [63].

The precision of the developed method was evaluated through repeatability (intra-day precision) with six experiments conducted on the same day and intermediate precision (inter-day precision) with three assays performed over five consecutive days for 5.15×10^{-7} mol dm^{-3} FA under optimal experimental conditions (refer to Table 1). The satisfactory recoveries indicate that the CPT-BDD electrode is a reliable electrochemical sensor for accurate quantification of FA in real samples.

To our knowledge, no study using bare electrodes for the determination of FA has been encountered thus far. Table 2 compares the analytical performance of the CPT-BDD electrode with that of carbon-based modified electrodes in previously published papers. These data highlight that the CPT-BDD electrode exhibits lower LOD compared to other electrodes, including the graphene nanosheets glassy carbon electrode (GN/GCE) [23], the

Table 1 Analytical parameters obtained for oxidation peak of FA using SWV on CPT-BDD electrode

Analytical parameter	
E_p	+0.82 V
LWR	0.1–8.0 mg dm^{-3} (5.15×10^{-7}–4.12×10^{-5} mol dm^{-3})
LRE	i_p/µA = 0.8403 C/mg dm^{-3} + 0.1725
r	0.999
LOQ	0.097 mg dm^{-3} (4.98×10^{-7} mol dm^{-3})
LOD	0.029 mg dm^{-3} (1.49×10^{-7} mol dm^{-3})
Intra-day repeatability (RSD%, $n=10$)	3.62
Inter-day repeatability (RSD%, $n=5$)	4.77

E_p peak potential, *LWR* linear working range, *LRE* linear regression equation, r correlation coefficient, *LOQ* limit of quantification, *LOD* limit of detection

Table 2 Evaluation of the CPT-BDD electrode versus other electrodes commonly used to measure FA

Analyte	Electrode	Linearity range/μM	LOD/μM	Sample	References
FA	MWCNT/GCE	10–5000	0.1	Drug	[22]
FA	GN/GCE	0.5–50	0.2	Drug	[23]
FA	*f*-MWCNT/MnO2/GCE	0.082–220	0.01	Serum	[24]
FA, CA	CNF/SPE	10–1000	0.233	Drug	[25]
FA	CNF-GNP/SPE	0.1–129.6	0.002	Cosmetic	[26]
FA	ERGO/GCE	0.084–38.9	0.02	Sinensis	[27]
FA	CPE/MWCNTs-Ag	0.04–1000	0.03	Urine and wine	[28]
FA	PDDA-G/GCE	0.089–52.9	0.044	Angelica sinens	[7]
FA	rGO–TiO2–GCE	1–300	0.154	Food	[29]
FA, SO_3^{2-}	MgO/SWCNTs–[Bmim][Tf2N]–CPE	0.009–450	0.003	Food	[30]
FA	GOs/MWCNTs/GCE	0.24–32	0.08	Drug	[31]
FA	PPy-MWCNTs/GCE	3.32–25.9	1.17	Popcorn	[32]
FA	DDAB/Nafion/CPE	2–120	0.39	Drug	[33]
FA	rG-CdO/MOITF/CPE	0.02–40	0.008	Food	[34]
FA	γ-$CoTe_2$/GCE	0.03–28.0	0.013	Cosmetic	[35]
FA	BDD	0.515–41.2	0.149	Cosmetic	This work

Analyte: *FA* Ferulic Acid, *CA* Caffeic Acid, SO_3^{2-} sulfite ions; Electrode: *MWCNT/GC* glassy carbon electrode modified with multi-walled carbon nanotube, *GN/G* graphene nanosheet glassy carbon electrode, *f-MWCNT/MnO2/GCE* multi-walled carbon nanotube/manganese dioxide with glassy carbon electrode, *CNF/SPE* carbon nanofiber-based screen-printed sensor, *CNF–GNP/SPE* nanofibers of carbon modified with gold nanoparticles with screen-printed electrode, *ERGO/GCE* graphene oxide modified with glassy carbon electrode, *CPE/MWCNTs–Ag* multi-walled carbon nanotube decorated with silver nanoparticles modified carbon paste electrode, *PDDA–G/GCE* graphene-modified glassy carbon electrode, *rGO–TiO_2–GCE* TiO_2 nanoparticles decorated, chemically reduced graphene oxide (rGO–TiO_2)-modified glassy carbon electrode, *MgO/SWCNTs–[Bmim][Tf_2N]–CPE* nanocomposite and 1-butyl-3-methylimidazolium bis(trifluoromethylsulfonyl)imide [Bmim][Tf_2N] into the carbon paste matrix; GOs/MWCNTs/GCE, graphene oxide sheets (GOs) and multi-walled carbon nanotubes (MWCNTs) nanocomposites modified glassy carbon electrode; *PPy-MWCNTs/GCE* polypyrrole-multi-walled carbon nanotubes with glassy carbon electrode, *DDAB/Nafion/CPE* didodecyldimethylammonium bromide/Nafion composite film-modified carbon paste electrode, *rG–CdO/MOITF/CPE* graphene decorated nanocomposite/1-methyl-3-octylimidazolium tetrafluoroborate ionic liquid carbon paste electrode, *γ-$CoTe_2$/GCE* γ-$CoTe_2$ nanocrystals modified glassy carbon electrode, *BDD* Boron-doped diamond electrode

carbon nanofiber-based screen-printed electrode (CNF/SPE) [25], the polypyrrole-multi-walled carbon nanotubes glassy carbon electrode (PPy-MWCNTs/GCE) [32], the TiO_2 nanoparticles decorated chemically reduced graphene oxide modified glassy carbon electrode (rGO–TiO_2–GCE) [29], and the didodecyldimethylammonium bromide/nafion composite film-modified carbon paste electrode (DDAB/Nafion/CPE) [33]. Conversely, several modified electrodes reported in the literature exhibit lower LOD values than the CPT-BDD electrode, such as the multi-walled carbon nanotube manganese dioxide glassy carbon electrode (*f*-MWCNT/MnO_2/GCE) [24], the nanofibers carbon-modified gold nanoparticles screen-printed electrode (CNF-GNP/SPE) [26], and other modified electrodes [7, 27, 28, 30, 31, 34, 35]. However, modified carbonaceous electrodes exhibit certain drawbacks, including prolonged preparation times, limited reproducibility, and high costs. In our study, utilizing the unmodified CPT-BDD electrode offers advantages in terms of simplicity, affordability, and efficiency, in contrast to studies involving modified electrodes within the literature.

Within the same experimental circumstances with a constant FA content (5.15×10^{-6} mol dm^{-3}), several ions and tiny biological molecules frequently discovered in cosmetic samples specimens were examined to verify the selectivity of the suggested approach. Zn^{2+}, Na^+, Ca^{2+}, Cu^{2+}, Ag^+, Cl^-, NO_3^-, fructose, lactose, and glucose, all at 100-fold surplus quantities, were found to have a minor effect on detecting FA. But the interferences of ascorbic acid, uric acid, and dopamine, which are usually found in urine, were also tested at molar concentrations of 1:1 (FA: interfering agent) to show that it is possible to track this compound in biological fluids for pharmacokinetic and pharmacodynamic studies. The oxidation signals of these substances coexisted with FA at similar oxidation potentials. On the other hand, potential interference arising from certain related phenolic compounds that might coexist with FA in various food samples was also examined. The coexistence of gallic acid,

chlorogenic acid, syringic acid, and caffeic acid resulted in overlapping signals on the CPT-BDD electrode, even when employing an analyte-to-interferent ratio of 1:1. Hence, the total content of the phenolic compounds could be assessed using the proposed methodology in relevant samples.

In light of these results, various standard addition method was used to analyze the FA content in the injection sample. The sample preparation and analysis processes are detailed in the Experiment Part. In Fig. 6, we have a graphical assessment of the standard addition method for the oxidation signal of FA, along with some example SW voltammograms of the sample.

Standard FA solutions made in a supporting electrolyte were added to 10 cm^3 of the sample solution in a voltammetric cell, and the voltammetric responses were measured to ensure the accuracy of the established approach for real-world applications. The percentage of recovered FA was determined by comparing the concentrations of the spiking and unadulterated substances. When sample dilutions were considered, it was found that the injectable solution tablet had 0.96 mg cm^{-3} (RSD = 3.5%) of FA, which is close to the 1.0 mg cm^{-3} label value indicated by the manufacturer. Table 3 displays the FA recovery values that were determined. As a result, the suggested technique provides assurance that the voltammetric quantification of FA in the commercial injection sample will be accurate.

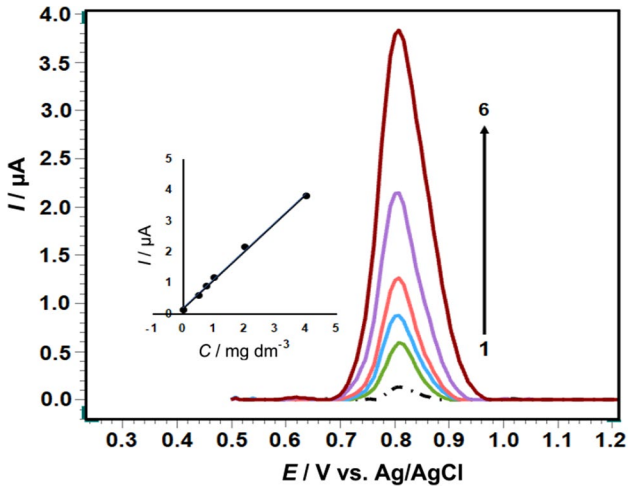

Fig. 6 SW voltammograms of the diluted ampule sample (dashed line) and after standard additions of 2.28×10^{-6}, 3.86×10^{-6}, 5.15×10^{-6}, 1.03×10^{-5}, and 2.06×10^{-5} mol dm^{-3} FA (1–5) in 0.1 mol dm^{-3} H_2SO_4. Analysis using the standard addition approach for the oxidation peak is shown in the inset. A variety of alternative operating circumstances are demonstrated in Fig. 5

Conclusions

This study appears to be detailing the electrochemical research of FA. For the purpose of voltammetrically determining FA, the CPT-BDD electrode, in combination with SWV, was investigated for its potential usefulness. The strategy that has been described has the potential to be immediately applicable to the routine quality monitoring of commercial products. This would eliminate the need for organic chemicals, complicated sample extraction methods, or pricey instruments.

Experimental

The FA reference standard was purchased from Sigma-Aldrich in its nearly perfect state (98%) and utilized without undergoing any additional purification steps. Since FA is poorly soluble in water, we made a stock solution by dissolving the desired amount in methanol and stored it in the fridge until we were ready to use it. The stock solution had a 5.15×10^{-3} mol dm^{-3} concentration. Sigma-Aldrich provided a purified version (> 98%) used directly from the container. The Britton–Robinson (BR) buffer was made with analytical-grade chemicals and extremely pure water supplied by the Milli-Q purification device (Millipore, resistivity 18.2 MΩ cm). The buffer had a concentration of 0.04 mol dm^{-3} in each of its constituents. These supportive electrolytes diluted FA working solutions to lower concentrations at specific pH levels. Voltammetric observations in aquatic buffer solutions were unaffected by the presence of methanol, which was maintained at a level of < 10% of the total volume in the voltammetric cell. Potassium chloride (KCl) and the probable interfering substances (ascorbic acid, uric acid fructose, glucose, lactose, and dopamine) were acquired from Sigma-Aldrich.

Table 3 Analysis of commercial injection sample spiked with FA standard solutions using SWV on cathodically pretreated BDD electrode

Added[a]/mol dm^{-3}	Expected[a]/mol dm^{-3}	Found[a,b]/mol dm^{-3}	Recovery ± RSD/%
0	–	7.11×10^{-7}	–
2.28×10^{-6}	2.99×10^{-6}	2.77×10^{-6}	92.6 ± 5.2
3.86×10^{-6}	4.57×10^{-6}	4.44×10^{-6}	97.2 ± 4.1
5.15×10^{-6}	5.86×10^{-6}	6.05×10^{-6}	103.5 ± 3.4

[a]Concentration in the measured solution

[b]Average of three replicate measurements

Apparatus and measurements

An Autolab electrochemical analyzer (Metrohm, The Netherlands) controlled with the NOVA 2.1.3 version was used for all of the voltammetric observations, including cyclic voltammetry (CV) and square-wave voltammetry (SWV). First, we used cyclic voltammetry (CV). Then, we systematically studied square-wave voltammetry (SWV) to determine the optimal circumstances for electroanalytical methods and to delve into the challenge of determining FA. After smoothing with a Savicky and Golay logarithm in NOVA 2.1.3 and performing a baseline correction using a moving average approach (peak width of 0.01 V), the voltammograms obtained with SWV were displayed. All voltammetric measurements were carried out in a glass electrochemical cell with a volume of ten milliliters and utilizing the conventional configuration of three electrodes. The platinum wire served as the counter electrode, whereas the reference electrode was a silver/silver chloride solution (3 mol dm^{-3} NaCl, Model RE-1, BAS, USA). Windsor Scientific Ltd. (UK) provided the commercially available BDD working electrode (diameter 3 mm, boron concentration 1000 ppm). Each day, the BDD electrode was immersed in 0.5 mol dm^{-3} H_2SO_4 and subjected to a cathodic potential of – 1.8 V for 180 s (to refresh the hydrogen-terminated electrode surface). Before beginning each voltammetric experiment, a cathodic potential of – 1.8 V was provided to the BDD electrode using the same solution for a period of 60 s in a 0.5 mol dm^{-3} H_2SO_4 solution. To determine the pH of the solution, a WTW inoLab pH 720 m outfitted with an additional electrode (glass-reference electrodes) was utilized. At the temperature of the laboratory, each measurement was carried out in triplicate (except for the repeatability evaluation).

Preparation of samples

A sample of FA injectable solution from a nearby beauty salon was manufactured commercially by Emfa medical cosmetics in Turkey and branded as containing 1 mg cm^{-3} FA. The necessary amount of this injectable solution was measured, then diluted with H_2SO_4 solution in a 25 cm^3 volumetric flask. After that, 0.25 cm^3 of this solution was added to the voltammetric cell, and then it was diluted to a total volume of 10 cm^3 using the supporting electrolyte. Additional dilutions were achieved through the sequential addition of standard solutions. The standard addition technique was used for the quantitative analysis.

Data availability All data generated in this study are available in this article and online supplementary material.

References

1. Zhang Y, Xu M, Du M, Zhou F (2007) Electrophoresis 28:1839
2. Tee-ngam P, Nunant N, Rattanarat P, Siangproh W, Chailapakul O (2013) Sensors 13:13039
3. Wang JZ, Yuan HP, Zhao DH, Ju YJ, Chen XY, Chen JP, Zhang J (2011) Ethnopharmacol 137:992
4. Lu GH, Chan K, Leung K, Chan CL, Zhao ZZ, Jiang ZH (2005) J Chromatogr A 1068:209
5. Graf E (1992) Free Radic Biol Med 13:435
6. Jadhav AP, Kareparamban JA, Nikam PH, Kadam VJ (2012) Pharm Sin 3:680
7. Liu LJ, Gao X, Zhang P, Feng SL, Hu FD, Li YD, Wang CM (2014) J Anal Methods Chem 2014:424790
8. Li LJ, Yu LB, Chen QF, Cheng H, Wu FM, Wu JL, Kong HX (2007) Chin J Anal Chem 35:933
9. Blasco AJ, González Crevillén A, González MC, Escarpa A (2007) Electroanalysis 19:2275
10. Arribas AS, Martinez-Fernandez M, Chicharro M (2012) TrAC Trends Anal Chem 34:78
11. Swaroop A, Bagchi M, Moriyama H, Bagchi D (2017) Sustained energy for enhanced human functions and activity. Academic Press, p 411
12. Karimi-Maleh H, Farahmandfar R, Hosseinpour R, Alizadeh J, Abbaspourrad A (2019) Chem Pap 73:2441
13. Berton SB, Cabral MR, de Jesus GA, Sarragiotto MH, Pilau EJ, Martins AF, Bonafe EG, Matsushita M (2020) Ind Crops Prod 154:112701
14. Xu Y, Lin D, Yu X, Xie X, Wang L, Lian L, Fei N, Chen J, Zhu N, Wang G, Huang X (2016) Oncotarget 7:20455
15. Bumrungpert A, Lilitchan S, Tuntipopipat S, Tirawanchai N, Komindr S (2018) Nutrients 10:713
16. Zheng Y, You X, Guan S, Huang J, Wang L, Zhang J, Wu J (2019) Adv Funct Mater 29:1808646
17. Mori T, Tsuchiya R, Doi M, Nagatani N, Tanaka T (2019) J Incl Phenom Macrocycl Chem 93:91
18. Romana-Souza B, Silva-Xavier W, Monte-Alto-Costa A (2020) J Cosmet Dermatol 19:2965
19. Brito LG, Leite GQ, Duarte FÍC, Ostrosky EA, Ferrari M, de Lima AAN, Nogueira FHA, Aragão CFS, Ferreira BDDL, de Freitas Marques MB, Yoshida MI (2019) J Therm Anal Calorim 138:3715
20. Chaudhary A, Jaswal VS, Choudhary S, Sharma A, Beniwal V, Tuli HS, Sharma S (2019) Recent Pat Inflamm Allergy Drug Discov 13:115
21. Zduńska K, Dana A, Kolodziejczak A, Rotsztejn H (2018) Skin Pharmacol Physiol 31:332
22. Yu YY, Wu QS, Wang XG, Ding YP (2009) Russ J Electrochem 45:170
23. Zhang Y, Liu Y, Yang Z, Yang Y, Pang P, Gao Y, Hu Q (2013) Anal Methods 5:3834
24. Vilian AE, Chen SM (2015) Microchim Acta 182:1103
25. Bounegru AV, Apetrei C (2022) Sensors 22:4689
26. Bounegru AV, Apetrei C (2020) Sensors 20:6724
27. Liu L, Gou Y, Gao X, Zhang P, Chen W, Feng S, Hu F, Li Y (2014) Mater Sci Eng C 42:227
28. Erady V, Mascarenhas RJ, Satpati AK, Detriche S, Mekhalif Z, Dalhalle J, Dhason A (2017) J Electroanal Chem 806:22
29. Bharathi TD, Anandh SP, Rangarajan M (2018) In: 2018 15th IEEE India Council International Conference (INDICON). IEEE
30. Zabihpour T, Shahidi SA, Karimi-Maleh H, Ghorbani-Hasan-Saraei A (2020) Microchem J 154:104572
31. Xia Z, Zhang Y, Li Q, Du H, Gui G, Zhao G (2020) Int J Electrochem Sci 15:559
32. Abdel-Hamid R, Newair EF (2015) Nanomaterials 5:1704

33. Luo L, Wang X, Li Q, Ding Y, Jia J, Deng D (2010) Anal Sci 26:907
34. Ebrahimi P, Shahidi SA, Bijad M (2020) J Food Meas Charact 14:3389
35. Malagutti MA, Ulbrich KF, Winiarski JP, Paes VZC, Geshev J, Jost CL, Campos CEM (2022) Mater Today Commun 31:103481
36. Marković D, Petranović NA, Baranac JM (2000) J Agric Food Chem 48:5530
37. Tian W, Chen G, Gui Y, Zhang G, Li Y (2021) Food Control 123:107691
38. Song-gang J, Yi-feng C, Yu-tian W, Xue-ping Y, Dong-sheng L, Zi-ming X, Xiao L (1999) Biomed Chromatogr 13:333
39. Mabinya LV, Mafunga T, Brand JM (2006). Afr J Biotechnol. https://doi.org/10.4314/ajb.v5i13.43097
40. Hingse SS, Digole SB, Annapure US (2014) J Anal Sci Technol 5:1
41. Nadal JM, Toledo MDG, Pupo YM, de Paula JP, Farago PV, Zanin SMW (2015) J Anal Methods Chem 2015:286812
42. Jankovska P, Copikova J, Sinitsya A (2001) Czech J Food Sci 19:143
43. Fu L, Chen Q, Chen J, Ren L, Tang L, Shan W (2021) J Chromatogr B 1180:122870
44. Li X, Li X, Wang L, Li Y, Xu Y, Xue M (2007) J Pharm Biomed Anal 44:1106
45. Yue Q, Yang HJ, Li DH, Wang JQ (2009) Anim Feed Sci Technol 153:169
46. Khezeli T, Daneshfar A, Sahraei R (2016) Talanta 150:585
47. Saini S, Sharma T, Patel A, Kaur R, Tripathi SK, Katare OP, Singh B (2020) J Chromatogr B 1155:122300
48. Traunmüller F, Steiner I, Zeitlinger M, Joukhadar C (2006) J Chromatogr B 843:142
49. Cinková K, Kianičková K, Stanković DM, Vojs M, Marton M, Švorc Ľ (2018) Anal Methods 10:991
50. Švorc Ľ, Jambrec D, Vojs M, Barwe S, Clausmeyer J, Michniak P, Marton M, Schuhmann W (2015) ACS Appl Mater Interfaces 7:18949
51. Kondo T (2022) Curr Opin Electrochem 32:100891
52. Ali HS, Barzani HA, Yardım Y (2022) Diam Relat Mater 123:108871
53. Barzani HA, Yardım Y (2023) Diam Relat Mater 132:109658
54. Švorc Ľ, Haššo M, Sarakhman O, Kianičkova K, Stanković DM, Otřísal P (2018) Microchem J 142:297
55. Barzani HA, Ali HS, Yardım Y (2023) Diam Relat Mater 132:109647
56. Cinková K, Švorc Ľ, Šatkovská P, Vojs M, Michniak P, Marton M (2016) Anal Lett 49:107
57. Hoshyar SA, Barzani HA, Yardım Y, Şentürk Z (2021) Colloids Surf A Physicochem Eng Asp 610:125916
58. Yence M, Cetinkaya A, Ozcelikay G, Kaya SI, Ozkan SA (2022) Crit Rev Anal Chem 52:1122
59. Sarakhman O, Švorc Ľ (2022) Crit Rev Anal Chem 52:791
60. Barzani HA, Ali HS, Özok Hİ, Yardım Y (2022) Diam Relat Mater 124:108934
61. Barzani HA, Saadi Ali H, Şahin C, Kıran M, Yardım Y (2022) Electroanalysis 34:1280
62. Ali HS, Barzani HA, Yardım Y (2023) Microchem J 189:108572
63. Gumustas M, Ozkan SA (2011) Open Anal Chem J 5:1